HHS Public Access

Author manuscript

Langmuir. Author manuscript; available in PMC 2017 March 29.

Published in final edited form as:

Langmuir. 2016 March 29; 32(12): 2874–2881. doi:10.1021/acs.langmuir.5b04540.

Role of Aromatic Interactions in Temperature-Sensitive Amphiphilic Supramolecular Assemblies

Oyuntuya Munkhbat[†], **Matteo Garzoni**[§], **Krishna R. Raghupathi**[†], **Giovanni M. Pavan**[§], and **S. Thayumanavan**[†]

Giovanni M. Pavan: giovanni.pavan@supsi.ch; S. Thayumanavan: thai@chem.umass.edu

[†]Department of Chemistry, University of Massachusetts, Amherst, MA 01003, United States

[§]Department of Innovative Technologies, University of Applied Sciences and Arts of Southern Switzerland, Galleria 2, Manno 6928, Switzerland

Abstract

Aromatic interactions were found to greatly influence the temperature-dependent dynamic behavior within supramolecular assemblies. Using an amphiphilic dendron, we systematically changed the hydrophobic groups introducing increasing levels of aromaticity while keeping the hydrophilic part constant. We show that the supramolecular assemblies become less sensitive to temperature changes when aromatic interactions in the aggregate are increased. Conversely, the absence of aromaticity in the hydrophobic moieties produces temperature-sensitive aggregates. These results show that subtle molecular-level interactions can be utilized to control temperature-sensitive behavior in the nanoscale. These findings open up new design strategies to rationally tune stimuli-responsive supramolecular assemblies on multiple spatiotemporal scales.

Graphical Abstract

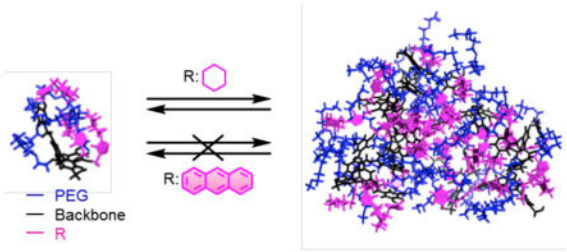

INTRODUCTION

Amphiphilic supramolecular assemblies have been of great interest due to their potential utility in a variety of applications such as drug delivery, biosensing and catalysis.[1–10] Understanding the molecular design elements that control not only the final macroscopic structural features, but also the dynamic properties of the assembly is critical in developing versatile new supramolecular assemblies. In this context, there is a notable interest in

Correspondence to: Giovanni M. Pavan, giovanni.pavan@supsi.ch; S. Thayumanavan, thai@chem.umass.edu.

temperature-sensitive systems, as these facilitate convenient extrinsic control over self-assembly.[11–17] Oligo- and poly-ethylene glycol (OEG and PEG) based systems have attracted considerable attention, because of their hydrogen bonding based interactions with water that affords temperature-dependent hydrophilicity.[18–20] In these cases, aggregation becomes stronger at higher temperatures,[21,22] because the loss of hydrogen bonding between the temperature-sensitive functionalities and water reduces the amphiphilie's hydrophilicity.[21–23] Thus, most of these sensitivities arise directly from the temperature-sensitive moiety itself. In this work, we show that aromatic interactions, which are tucked within the interiors of the assembly,[24,25] can also play a fundamental role in controlling the temperature-sensitive behavior of supramolecular assemblies (Figure 1).

To evaluate the role of aromatic interactions on the temperature-sensitive self-assembly, we designed facially amphiphilic dendrons with variable levels of aromaticity (Scheme 1). Dendrimers and dendrons are interesting platforms for this study, as these combine the advantages of small molecule amphiphiles in that they are structurally well-defined and polymers in that they are characterized by high thermodynamic stabilities.[26–35] The targeted aromatic hydrophobic units include phenyl, naphthyl, and anthracyl moieties, having an increasing trend in hydrophobicity as well as aromaticity. Cyclohexyl provides a useful comparison with a non-aromatic hydrophobic unit with similar geometry and rigidity. To ensure uniformity, the dendrons were prepared using a modular approach, where the hydrophobic group was 'clicked' on to propargyl moieties.

EXPERIMENTAL METHODS

Preparation of dendrimer solutions

Stock solution (100 μM) of each dendrimer was prepared by dissolving the dendrimer in milli-Q water at room temperature. Solutions were sonicated for 3 hours, and stirred at 4 °C for one week ahead of any experiment. Dendrimer solutions were diluted to required concentrations before each experiment.

Dynamic light scattering (DLS) measurements

The size distribution of the aggregates were determined by Malvern Zetasizer (Nano-ZS). For each DLS experiment, 100 μM solution was diluted to 25 μM and filtered through 0.45 μm filter. Hydrodynamic radius (DH) of the dendritic assembly was measured at different temperatures with 7 minutes of equilibration time to achieve desired temperature before each measurement and repeated in triplicate. Size distribution, correlograms and PDI for all samples can be found in the supporting information (Figure S1, Figure S2, Figure S3 and Table S1).

Dye encapsulation and guest exchange study

To a vial containing 1.2 mL of 25 μM dendrimer solution added 2 μL of 0.77 mg/mL pyrene (in acetone) and perylene (in acetone) separately, followed by evaporation of acetone by leaving the vial uncapped for 30 minutes while stirring at room temperature. After 30 min, the vial is capped and solution was stirred for 24 hours at room temperature. FRET experiments were performed on a JASCO (PF-6500) spectrofluorimeter and UV-Vis spectra

were collected using a Cary-100 scan spectrophotometer. FRET measurements started as soon as pyrene and perylene containing dendrimer solutions (25 μM) were mixed (1:1 by volume). Pyrene was excited at 339 nm, pyrene and perylene emission were monitored at 375 and 447 nm respectively for the calculation of FRET ratio.

Time-dependent fluorescence and host exchange

Time-lapse studies were performed on a PTI Quantamaster-30 phosphorescence/ fluorescence spectrofluorimeter with a xenon flash power supply and TC125 temperature controller. Host exchange experiment of each dendron (CHE, PHE, NAP, and ANT) with pyrene dendrimer, Pyr, was performed at 5 °C, 10 °C, 25 °C and 40 °C. Dendrimer solutions (25 μM) were pre-equilibrated at target temperature 1 °C for 30 min prior to mixing. 0.5 mL of Pyr solution was added to a fluorescence cuvette in a thermoelectric cuvette holder and allowed to equilibrate. 0.5 mL of CHE was added through syringe directly into the cuvette and emission at 379 nm was monitored with time. Instrument parameters were adjusted at 339 nm for excitation and 379 nm for emission. Sample was being stirred at low rpm during the measurement. Same procedure was followed for all other dendrons (PHE, NAP, and ANT).

RESULTS AND DISCUSSION

Synthesis

We designed the dendrons such that these molecules can be synthesized using a modular approach, providing facile access to the target molecules. To achieve this, we used the G1 dendritic scaffold with propargyl functionalities at every repeat unit of the dendron, shown as structure **8** in Scheme 2. This functional group was used as the handle to simply vary the hydrophobic functional groups using the Hüisgen-1,3-dipolar cycloaddition reaction, the so-called click chemistry.[36–40] Module **8** was prepared by reacting the biaryl molecule **6** with the 3,5-dialkoxybenzyl bromide **7** in the presence of potassium carbonate and 18-crown-6, as shown in Scheme 2. All the targeted dendrons were successfully obtained using the copper-catalyzed click reaction between the propargyl core **8** and the azide functionalized alkyl or aryl-substituted substrates **9**–**12** (see Supporting Information for synthetic details and characterizations). The alkyl azides used in the click reaction were obtained from the corresponding alkyl bromides by reaction with sodium azide.

Aggregation Behavior

First, we evaluated the self-assembly formation of each of these dendrons in water. Since the critical aggregation concentrations of all these dendrons were well below 25 μM (Figure S5), all dendrons were assembled at this concentration. The sizes of the assemblies were found to range between 150 and 180 nm at room temperature (Figure 2a), as discerned by dynamic light scattering (DLS) measurements with good correlation functions (>0.85) and dispersities (0.04 and 0.18). We found that the all of the dendrons form spherical micelle-like assemblies in water (See SI for TEM images, Figure S4).

The sizes of these assemblies were then evaluated at different temperatures. Interestingly, a significant size reduction from 181 nm at 25 °C to 95 nm at 5 °C was observed for the

cyclohexyl dendron (CHE) (Figure 2b). This is reminiscent of the recently reported sub-LCST transition.[41,42] The results in Figure 2c show that the structural transition is most significant at ~18 °C for CHE dendron. The phenyl dendron (PHE) also presents a structural transition at ~6 °C. Interestingly, naphthyl (NAP) and anthracyl (ANT) dendrons do not exhibit any sub-LCST transitions, even though they also contain PEG groups. These observations provided the first indications that the nature of the hydrophobic substituents might have a significant influence over the thermal-sensitive behavior of these supramolecular assemblies, and that the latter cannot be simply explained by hydrophilic-lipophilic balance (HLB) variations – the behavior of the different aggregates do not have a direct correlation with the *log P* of the substituents (Scheme 1).

Temperature-Dependent Exchange of Dendrons

We tested whether these temperature-sensitive transitions could be related to a differential stability of the dendritic assemblies. Thanks to a recently reported time-lapse fluorescence method, which used a pyrene-labeled dendron (Pyr) as the fluorescent probe (Figure 3a and 3b),[41] we assessed the residence time of the dendrons into the aggregate, and the dynamic exchange of dendrons with the solution. Briefly, Pyr exhibits significant excimer emission in the assembled state, as the local concentration of the pyrene within the assembly interior is very high. If Pyr aggregates are mixed in solution with the other assemblies (CHE, PHE, NAP or ANT), a change in the pyrene fluorescence properties indicates that the dendrons can exchange dynamically between the aggregates in solution (Figure 3c). We tracked the increase in monomer emission intensity at 379 nm with time-lapse fluorescence spectroscopy upon mixing of Pyr dendron with other dendrons (CHE, PHE, NAP and ANT), while varying the temperature. Aqueous solutions of the dendrons (25 μM) were pre-equilibrated at the desired temperature for 30 min and then mixed in a cuvette for immediate fluorescence measurement. For all trials, pre-measurement of pyrene dendron solution alone was provided for few seconds prior to the addition of the mixing dendron to ensure that there was no monomer emission initially. This setup allowed us to study whether the monomer exchange dynamics of these assemblies vary with the solution temperature.

First, we compared the CHE and the PHE dendrons. These are geometrically similar, but cyclohexyl units are more hydrophobic than phenyl units (see *log P* values in Scheme 1), while they lack aromaticity. The data in Figure 3d and 3e clearly show that both dendrons exhibit faster dendron exchange at 5 °C than at 25 °C. Overall, the exchange dynamics of CHE is faster than that of PHE. Interestingly, the effect of changing the temperature on the assembly dynamics (temperature-sensitivity) is also stronger for the CHE than for the PHE dendron. NAP dendron is expected to be more hydrophobic than PHE and similar to CHE based on the *log P* of the hydrophobic moieties (Scheme 1). Nevertheless, although the hydrophobic moieties of the self-assembling dendrons possess comparable hydrophobicity, the dynamics of NAP aggregates was found to be less sensitive to temperature changes compared to that of CHE (Figure 3f and 3d) and similar to that of PHE (see Figure 3f and 3e). These outcomes suggest that hydrophobicity itself is not the unique factor in controlling the assembly property and that aromatic interactions, which include π-π and van der Waals interactions, can play a major role in supramolecular structure and dynamics. Remarkably, the most hydrophobic and aromatic dendron ANT was found to be not dynamic at any of the

temperatures studied, and the most insensitive to temperature variations (Figure 3g). Conversely, the assembly of non-aromatic CHE is the most sensitive one to temperature variations, and the most dynamic one. The dynamic behavior of the aggregate seems to become less temperature-sensitive, while the aromaticity of the dendrons is increased.

Guest Exchange Properties

Given that the exchange properties of these dendrons vary, it is interesting to investigate whether a similar trend, dominated by aromatic interactions, would be observed with guest exchange in those assemblies. Note that these amphiphilic assemblies can be hosts for non-covalently binding hydrophobic guest molecules in the aqueous phase. To test whether the trend exists, we used a recently developed fluorescence resonance energy transfer (FRET) based method to acquire guest exchange dynamics (Figure 4a).[43] For this study, we used pyrene and perylene as the hydrophobic FRET pair (see SI for experimental details). We notice that the CHE dendron exhibited the fastest guest exchange, whereas there was essentially no FRET observed for ANT dendron, suggesting that the exchange dynamics in aromatic dendron assemblies are in general slower than the non-aromatic CHE dendron (Figure 4b). There was a systematic trend in guest exchange dynamics of aromatic dendrons from PHE to NAP to ANT, which suggests that the stability of the assembly (as determined by the guest encapsulation stability) increases with increasing size of the aromatic side chain functionality. All these data are consistent with the host exchange properties observed previously and highlight the importance of understanding host exchange dynamics in amphiphilic supramolecular assemblies.

Molecular Dynamics (MD) Simulation Study

Important questions remain open on the origin of the temperature-sensitivity in the dendron aggregates. This is probably due to the interactions between the hydrophobic moieties inside the aggregates: the real variables in this study. However, aromatic and hydrophobic interactions are unavoidably interconnected in the tail-tail self-assembly in the real system. We have used all-atom molecular dynamics (MD) simulations to obtain molecular-level details of the dendron self-assembly in solution. First, we built and pre-equilibrated the single dendrons in water solution (see SI for computational details). Then, according to the same procedure used for similar facially amphiphilic dendrons and polymers in solution,[44,45] nine dendrons of each type were immerged in a periodic simulation box filled with water molecules (Figure 5a). MD simulations were carried out at 25 and 5 °C for each system to study aggregation at different experimental temperatures. All systems were simulated for 200 ns in NPT conditions. During this time, the dendrons self-assembled and all systems reached the equilibrium in the MD regime (see SI for details). The evolution of the radius of gyration (Rg) of the aggregates, of the PEG chains and of the hydrophobic groups during the MD simulations (Figure 5) shows that, the aggregates tend to converge to an equilibrated configuration where the hydrophilic PEG surrounds the hydrophobic groups to minimize the interaction with the solvent. While full reorganization into an ideal micelle-like aggregate is awkward for ANT and NAP structures due to the size and rigidity of the tail groups (Figure 5), ordered stacking of hydrophobic groups appears in many regions of the assembly (e.g., green ANT groups).

Enthalpy H as measured from the MD simulations is a good indicator of molecular solubility/hydrophobicity (see SI for comparison with log P).[46] According to a validated approach,[44,45] from the MD simulations we extracted the self-assembly enthalpy variations (ΔH) for each system at 5 °C and 25 °C (Table 1). While the ΔH values may depend on the flexibility of the different dendron architectures, it is not really informative to compare the ΔH of the different systems, but rather it is interesting to compare the ΔH of the same system at the two different T: $\Delta\Delta H = \Delta H$ (25 °C) – ΔH (5 °C). The $\Delta\Delta H$ values in Table 1 show that some assemblies are temperature sensitive and others are not – the more negative is the $\Delta\Delta H$ value, stronger is the interaction between the dendrons in the aggregates at high (25 °C) rather than at low temperature (5 °C).

$\Delta\Delta H$ is negligible for the more aromatic dendrons (NAP and ANT), whereas it is as high as −16 kcal/mol for the non-aromatic dendron CHE. The PHE system seems somewhat intermediate, with reduced, yet non-negligible, $\Delta\Delta H$ (−3.7 kcal/mol), and consistent with the temperature-dependent size transition and dendron exchange dynamics seen the experiments. In general, hydrophobic aggregation becomes stronger at higher T, which is the case for the non-aromatic CHE. However, the MD data in Table 1 show that over a certain level of aromaticity in the hydrophobic groups, the dendron interaction into the aggregates is not temperature-sensitive.

We were then interested in understanding how much of the self-assembly is directly imputable to hydrophobic tails of the dendrons: the real structural variables in this study. The radial distribution functions, *g(r)*, of the tail groups extracted from the MD simulations provide information on the interaction between the hydrophobic groups in the assembly (Figure 6). The higher and sharper the *g(r)* peak at short distance, the stronger the tail-tail interaction (*i.e.*, coordination, stacking). The related tail-tail interaction free energies (ΔE_{tail}) reported in Table 2 were obtained for all systems from the *g(r)* curves (see SI for details).[44] The ΔE_{tail} values show that the tail-tail interaction becomes stronger and temperature-insensitive for increasing levels of aromaticity. ΔE_{tail} is stronger at 25 °C than at 5 °C only for the non-aromatic system (CHE).

While the ΔE_{tail} energies include both hydrophobic and aromatic interactions, it is interesting to know how much of the tails interaction is directly imputable to the aromatic (only short-range) rather than to hydrophobic effects. The short-range aromatic contribution to self-assembly (ΔE_{stack}) was calculated as the number of stably stacked groups in the assemblies multiplied by the stacking interaction energies of CHE, PHE, NAP and ANT groups[47] respectively (see SI for details), according to the same approach adopted recently to quantify the role of hydrogen bonding in supramolecular polymers.[48] The remaining part of the tail-tail self-assembly energy (ΔE_{tail}) was assumed to be imputable to hydrophobic effect (ΔE_{hyd}). This analysis provides qualitative insight on the type of interactions in the self-assembly and on their modulation in response to temperature change.

The short-range tail-tail interactions (ΔE_{stack}) contribute only by 27–35% to the global tail-tail interaction in the CHE system, indicating the predominantly hydrophobic nature of the self-assembly in this case (Table 2). The long-range hydrophobic tail-tail interaction (ΔE_{hyd}), 2–3 times stronger than ΔE_{stack} in CHE, is also found to be temperature-sensitive

(ΔE_{hyd}: −25.3 vs. −32.3 kcal/mol at 5 and 25 °C respectively). Conversely, in the cases where the tail groups are aromatic (PHE, NAP and ANT), the short-range interactions (ΔE_{stack}) dominate the tails self-assembly (Table 2: ΔE_{stack} is ≈ 86%–98% of the total ΔE_{tail}), all terms are found to be substantially invariant on temperature changes. These observations clearly suggest that the dominance of aromatic interactions in these three dendrons substantially reduces the overall temperature sensitivity of these supramolecular assemblies.

Conclusions

In summary, we have systematically probed the hydrophobic moiety of the facially amphiphilic dendron while keeping the hydrophilic component unchanged in order to understand the influence of aromatic functional groups in controlling the temperature-responsive behavior of amphiphilic assemblies. Our combined experimental-theoretical approach provides a multiscale picture of these self-assembled materials in solution. We demonstrate that the inclusion of an increasing degree of aromaticity in the hydrophobic moieties of the self-assembling dendrons produces temperature-insensitive supramolecular assemblies, regardless of the level of the side chain hydrophobicity. On the other hand, when the hydrophobic groups of the dendrons lack aromaticity, the self-assembly is mainly controlled by hydrophobic interactions and the supramolecular material possesses a temperature-sensitive behavior. This study demonstrates how subtle changes in the self-assembling structures can produce different structural and dynamic properties on the supramolecular material. As amphiphilic assemblies are pursued in a variety of applications that require kinetic stability, such as in drug delivery or sensing, the design guidelines that emanate from this study will have broad implications.

Supplementary Material

Refer to Web version on PubMed Central for supplementary material.

References

1. Torchilin VP. Multifunctional, Stimuli-Sensitive Nanoparticulate Systems for Drug Delivery. Nat Rev Drug Discov. 2014; 13:813–827. [PubMed: 25287120]
2. Kataoka K, Harada A, Nagasaki Y. Block Copolymer Micelles for Drug Delivery: Design, Characterization and Biological Significance. Adv Drug Delivery Rev. 2001; 47:113–131.
3. Kelley EG, Albert JNL, Sullivan MO, Epps TH III. Stimuli-Responsive Copolymer Solution and Surface Assemblies for Biomedical Applications. Chem Soc Rev. 2013; 42:7057–7071. [PubMed: 23403471]
4. Soussan E, Cassel S, Blanzat M, Rico-Lattes I. Drug Delivery by Soft Matter: Matrix and Vesicular Carriers. Angew Chem Int Ed. 2009; 48:274–288.
5. Yao J, Yang M, Duan Y. Chemistry, Biology, and Medicine of Fluorescent Nanomaterials and Related Systems: New Insights into Biosensing, Bioimaging, Genomics, Diagnostics, and Therapy. Chem Rev. 2014; 114:6130–6178. [PubMed: 24779710]
6. Wang Y, Zhou K, Huang G, Hensley C, Huang X, Ma X, Zhao T, Sumer BD, DeBerardinis RJ, Gao J. A Nanoparticle-Based Strategy for the Imaging of a Broad Range of Tumours by Nonlinear Amplification of Microenvironment Signals. Nat Mat. 2014; 13:204–212.

7. Savariar EN, Ghosh S, Gonzalez DC, Thayumanavan S. Disassembly of Noncovalent Amphiphilic Polymers with Proteins and Utility in Pattern Sensing. J Am Chem Soc. 2008; 130:5416–5417. [PubMed: 18384200]
8. Peters RJRW, Marguet M, Marais S, Fraaije MW, van Hest JCM, Lecommandoux S. Cascade Reactions in Multicompartmentalized Polymersomes. Angew Chem Int Ed. 2014; 53:14–150.
9. Romsted LS, Bunton CA, Yao J. Micellar Catalysis, a Useful Misnomer. Curr Opin Colloid and Interface Sci. 1997; 2:622–628.
10. Astruc D, Chardac F. Dendritic Catalysts and Dendrimers in Catalysis. Chem Rev. 2001; 101:2991–3024. [PubMed: 11749398]
11. Lutz JF. Polymerization of Oligo(Ethylene Glycol) (Meth)Acrylates: Toward New Generations of Smart Biocompatible Materials. J Polym Sci Part A: Polym Chem. 2008; 46:3459–3470.
12. Lutz JF, Weichenhan K, Akdemir O, Hoth A. About the Phase Transitions in Aqueous Solutions of Thermoresponsive Copolymers and Hydrogels Based on 2-(2-methoxyethoxy)ethyl Methacrylate and Oligo(ethylene glycol) Methacrylate. Macromolecules. 2007; 40:2503–2508.
13. Inoue T, Matsuda M, Nibu Y, Misono Y, Suzuki M. Phase Behavior of Heptaethylene Glycol Dodecyl Ether and Its Aqueous Mixture Revealed by DSC and FT-IR Spectroscopy. Langmuir. 2001; 17:1833–1840.
14. Lutz JF, Hoth A. Preparation of Ideal PEG Analogues with a Tunable Thermosensitivity by Controlled Radical Copolymerization of 2-(2-Methoxyethoxy)ethyl Methacrylate and Oligo(ethylene glycol) Methacrylate. Macromolecules. 2006; 39:893–896.
15. Grzelczak M, Vermant J, Furst EM, Liz-Marzan LM. Directed Self-Assembly of Nanoparticles. ACS Nano. 2010; 4:3591–3605. [PubMed: 20568710]
16. Yong Yao Y, Xue M, Chen J, Zhang M, Huang F. An Amphiphilic Pillar[5]arene: Synthesis, Controllable Self-Assembly in Water, and Application in Calcein Release and TNT Adsorption. J Am Chem Soc. 2012; 134:15712–15715. [PubMed: 22967168]
17. Chi X, Ji X, Xia D, Huang F. A Dual-Responsive Supra-Amphiphilic Polypseudorotaxane Constructed from a Water-Soluble Pillar[7]arene and an Azobenzene-Containing Random Copolymer. J Am Chem Soc. 2015; 137:1440–1443. [PubMed: 25590459]
18. Hey MJ, Ilett SM. Poly(ethylene oxide) Hydration Studied by Differential Scanning Calorimetry. J Chem Soc Faraday Trans. 1991; 87:3671–3675.
19. Lüsse S, Arnold K. The Interaction of Poly(ethylene glycol) with Water Studied by ^{1}H and ^{2}H NMR Relaxation Time Measurements. Macromolecules. 1996; 29:4251–4257.
20. Vancoillie G, Frank D, Hoogenboom R. Thermoresponsive Poly(oligo ethylene glycol acrylates). Prog Poly Sci. 2014; 39:1074–1095.
21. Chandler D. Interfaces and the Driving Force of Hydrophobic Assembly. Nature. 2005; 437:640–647. [PubMed: 16193038]
22. Baldwin RL. Temperature Dependence of the Hydrophobic Interaction in Protein Folding. Proc Natl Acad Sci. 1986; 83:8069–8072. [PubMed: 3464944]
23. Holmberg, K.; Jonsson, B.; Kronberg, B.; Lindman, B. Surfactants and Polymers in Aqueous Solution. 2. J. Wiley; New York: 2002.
24. Tanford, C. The Hydrophobic Effect: Formation of Micelles and Biological Membranes. 2. J. Wiley and Sons; New York: 1980.
25. Israelachvili JN, Mitchell DJ, Ninham BW. Theory of Self-Assembly of Hydrocarbon Amphiphiles into Micelles and Bilayers. J Chem Soc, Faraday Trans 2. 1976; 72:1525–1568.
26. Fréchet JMJ. Dendrimers and Supramolecular Chemistry. Proc Nat Acad Sci. 2002; 99:4782–4787. [PubMed: 11959930]
27. Newkome GR, Moorefield CN. From 1→3 Dendritic Designs to Fractal Supramacromolecular Constructs: Understanding the Pathway to the Sierpiński Gasket. Chem Soc Rev. 2015; 44:3954–3967. [PubMed: 25316287]
28. Mignani S, El Kazzouli S, Bousmina MM, Majoral JP. Dendrimer Space Exploration: An Assessment of Dendrimers/Dendritic Scaffolding as Inhibitors of Protein–Protein Interactions, a Potential New Area of Pharmaceutical Development. Chem Rev. 2014; 114:1327–1342. [PubMed: 24127777]

29. Rosen, Brad M.; Wilson, Christopher J.; Wilson, Daniela A.; Peterca, Mihai; Imam, Mohammad R.; Percec, V. Dendron-Mediated Self-Assembly, Disassembly, and Self-Organization of Complex Systems. Chem Rev. 2009; 109:6275–6540. [PubMed: 19877614]
30. Moorefield, CN.; Perera, S.; Newkome, GR. Dendron Chemistry: Supramolecular Perspectives and Applications. John Wiley & Sons; Hoboken: 2012. p. 1-54.
31. Astruc D, Boisselier E, Ornelas C. Dendrimers Designed for Functions: From Physical, Photophysical, and Supramolecular Properties to Applications in Sensing, Catalysis, Molecular Electronics, Photonics, and Nanomedicine. Chem Rev. 2010; 110:1857–1959. [PubMed: 20356105]
32. Raghupathi K, Guo J, Munkhbat O, Rangadurai P, Thayumanavan S. Supramolecular Disassembly of Facially Amphiphilic Dendrimer Assemblies in Response to Physical, Chemical, and Biological Stimuli. Acc Chem Res. 2014; 47:2200–2211. [PubMed: 24937682]
33. Zimmerman SC, Lawless LJ. Supramolecular Chemistry of Dendrimers. Top Curr Chem. 2001; 217:95–120.
34. Kanna RM, Nance E, Kannan S, Tomalia DA. Emerging Concepts in Dendrimer-Based Nanomedicine: From Design Principles to Clinical Applications. J Int Med. 2014; 276:579–617.
35. Newkome GR, Moorefield CN, Baker GR, Saunders MJ, Grossman SH. Unimolecular Micelles. Angew Chem Int Ed. 1991; 30:1178–1180.
36. Lowe AB. Thiol-yne 'Click'/Coupling Chemistry and Recent Applications in Polymer and Materials Synthesis and Modification. Polymer. 2014; 55:5517–5549.
37. Xi W, Scott TF, Kloxin CJ, Bowman CN. Click Chemistry in Materials Science. Adv Func Mater. 2014; 24:2572–2580.
38. Iha RK, Wooley KL, Nystrom AM, Burke DJ, Kade MJ, Hawker CJ. Applications of Orthogonal "Click" Chemistries in the Synthesis of Functional Soft Materials. Chem Rev. 2009; 109:5620–5686. [PubMed: 19905010]
39. Kose MM, Onbulak S, Yilmaz II, Sanyal A. Orthogonally "Clickable" Biodegradable Dendrons. Macromolecules. 2011; 44:2707–2714.
40. Yesilyurt V, Ramireddy R, Thayumanavan S. Photoregulated Release of Noncovalent Guests from Dendritic Amphiphilic Nanocontainers. Angew Chem Int Ed. 2011; 123:3094–3098.
41. Fuller JM, Raghupathi KR, Ramireddy RR, Subrahmanyam AV, Yesilyurt V, Thayumanavan S. Temperature-Sensitive Transitions below LCST in Amphiphilic Dendritic Assemblies: Host–Guest Implications. J Am Chem Soc. 2013; 135:8947–8954. [PubMed: 23692369]
42. Raghupathi KR, Sridar U, Byrne AK, Thayumanavan S. Influence of Backbone Conformational Rigidity in Temperature-Sensitive Amphiphilic Supramolecular Assemblies. J Am Chem Soc. 2015; 137:5308–5311. [PubMed: 25893806]
43. Jiwpanich S, Ryu JH, Bickerton S, Thayumanavan S. Noncovalent Encapsulation Stabilities in Supramolecular Nanoassemblies. J Am Chem Soc. 2010; 132:10683–10685. [PubMed: 20681699]
44. Torres DA, Garzoni M, Subrahmanyam AV, Pavan GM, Thayumanavan S. Protein-Triggered Supramolecular Disassembly: Insights Based on Variations in Ligand Location in Amphiphilic Dendrons. J Am Chem Soc. 2014; 136:5385–5399. [PubMed: 24641469]
45. Kasimova AO, Pavan GM, Danani A, Mondon K, Cristiani A, Scapozza L, Gurny R, Moeller M. Validation of a Novel Molecular Dynamics Simulation Approach for Lipophilic Drug Incorporation into Polymer Micelles. J Phys Chem B. 2012; 116:4338–4345. [PubMed: 22435641]
46. Enciso AE, Garzoni M, Pavan GM, Simanek EE. Influence of Linker Groups on the Solubility of Triazine Dendrimers. New J Chem. 2015; 39:1247–1252.
47. Grimme S. Do Special Noncovalent π–π Stacking Interactions Really Exist. Angew Chem Int Ed. 2008; 47:3430–3434.
48. Baker MB, Albertazzi L, Voets IK, Leenders CMA, Palmans ARA, Pavan GM, Meijer EW. Consequences of Chirality on the Dynamics of a Water-Soluble Supramolecular Polymer. Nat Comm. 2015; 6:6234.

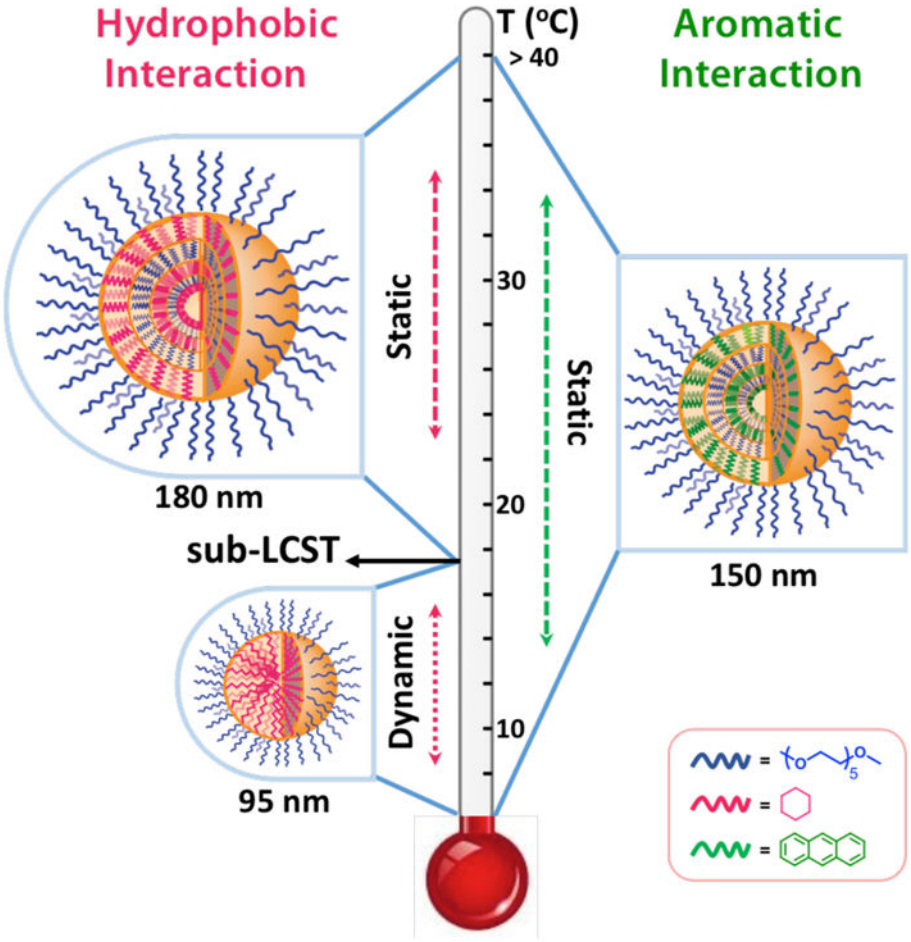

Figure 1.
Schematic presentation of temperature dependent size transition of amphiphilic assemblies, and role of aromaticity in this phenomenon.

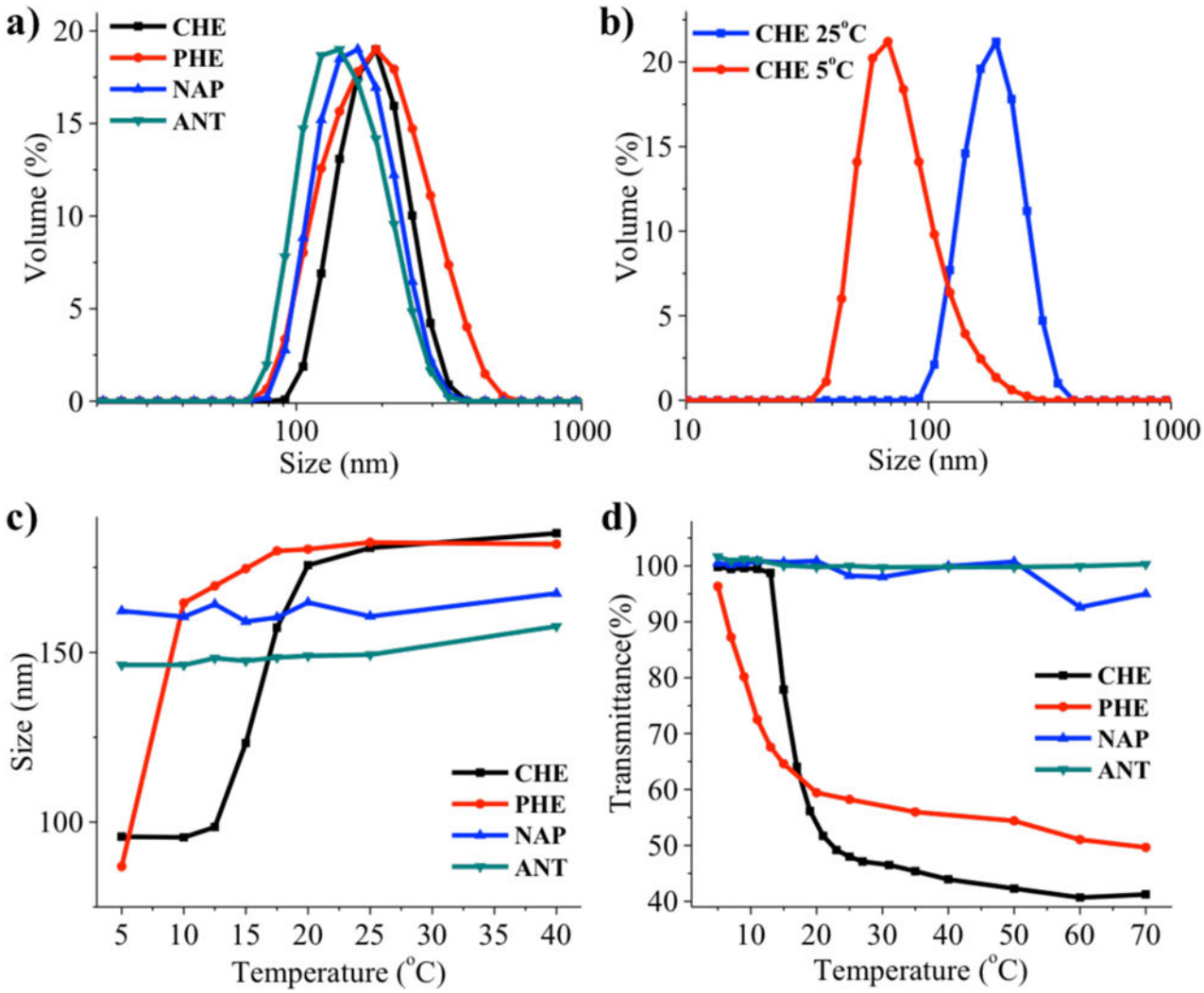

Figure 2.

a) DLS results of the assemblies formed from all dendrons at 25 °C; b) Size change for **CHE** dendron assembly at 25 °C (181 nm) and 5 °C (95 nm); c) Temperature dependent DLS measurement for all dendrons from 40 °C to 5 °C; d) Temperature dependent transmittance for all dendrons from 70 °C to 5 °C.

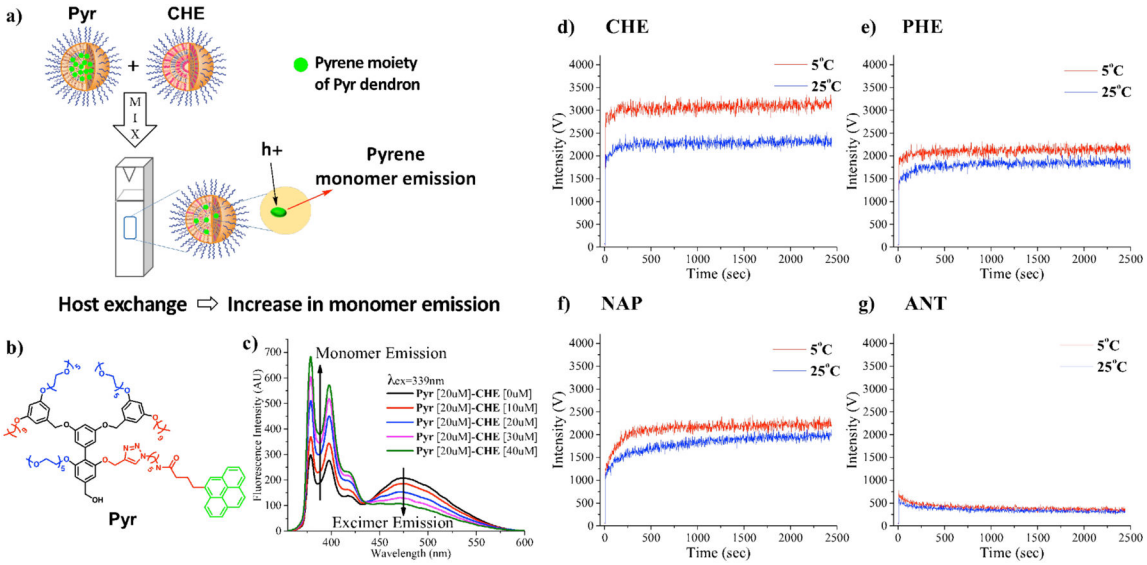

Figure 3.

a) Graphical illustration of dendron exchange experiment between **Pyr** and **CHE**. b) Structure of dendron **Pyr**; c) Evolution of pyrene monomer and pyrene excimer emission of dendron **Pyr** due to the dendron exchange with different concentrations of **CHE** Dendron; d–g) Time-based fluorescence measurement to monitor dendron exchange property of each dendron with fluorescent-labeled dendron **Pyr** by tracking pyrene monomer emission (379 nm) at 5 °C and 25 °C: d) **CHE**; e) **PHE**; f) **NAP**; g) **ANT**

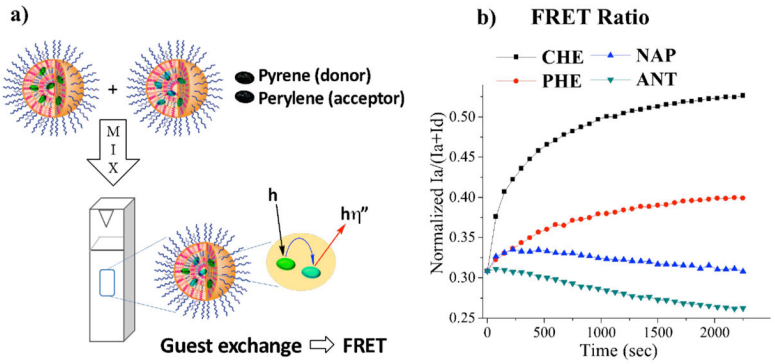

Figure 4.

a) Guest exchange experiment using pyrene and perylene; b) Normalized FRET ratio of all dendrons at 25 °C.

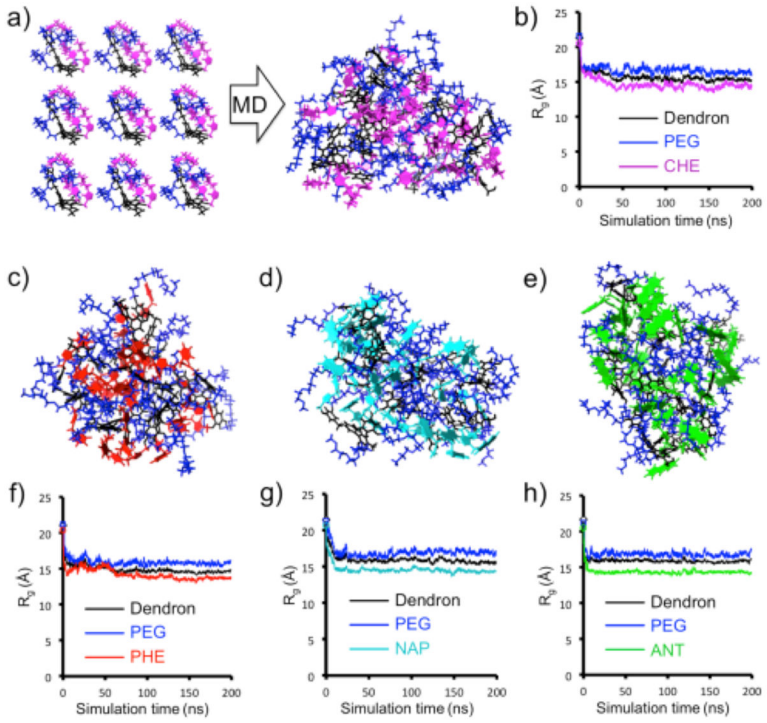

Figure 5.

Modeling dendrons self-assembly in solution. (a,c) Starting and equilibrated configuration of nine **CHE** in solution (PEG: blue, dendron scaffold: black, **CHE**: magenta). (c,d,e) Equilibrated configuration for the **PHE** (c: red), **NAP** (d: cyan), and **ANT** (d: green). (b,f,g,h) Radius of gyration (R_g) data of different groups of the dendrons as a function of simulation time.

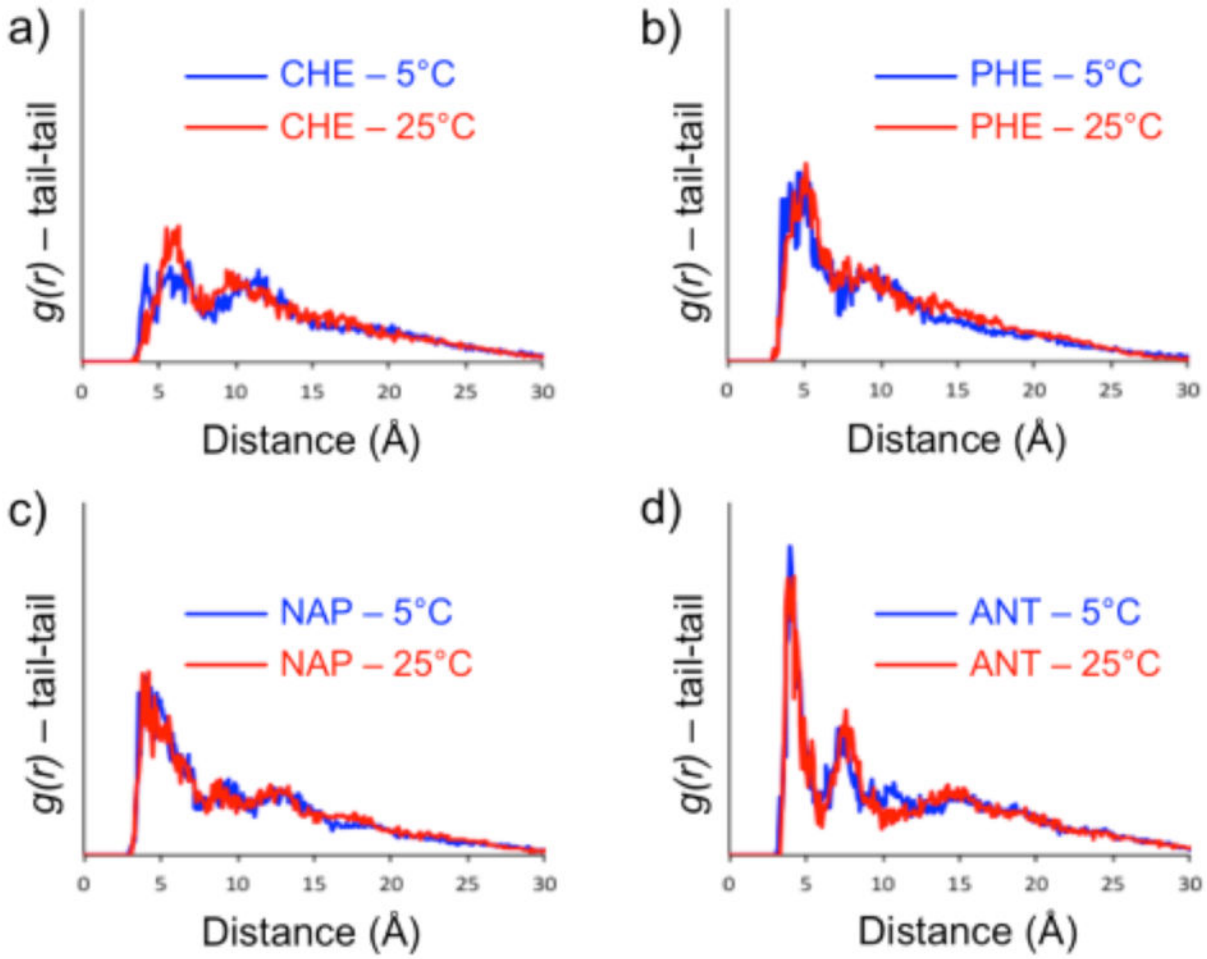

Figure 6.

Tail-tail self-assembly interaction. (a–d) Radial distribution functions – *g(r)* – of the tail groups respect to each other in the aggregates at 5°C (blue) and 25°C (red). High and sharp peaks at short distance identify stable and strong interaction (coordination/stacking).

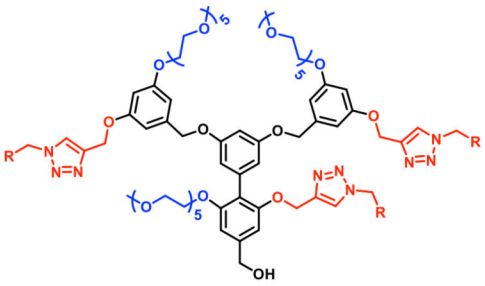

Dendron	R group	*log P*
CHE		*3.21*
PHE		*1.94*
NAP		*3.15*
ANT		*4.30*

Scheme 1.

Structures of the amphiphilic dendrons and the *log P* values of hydrophobic functional groups.

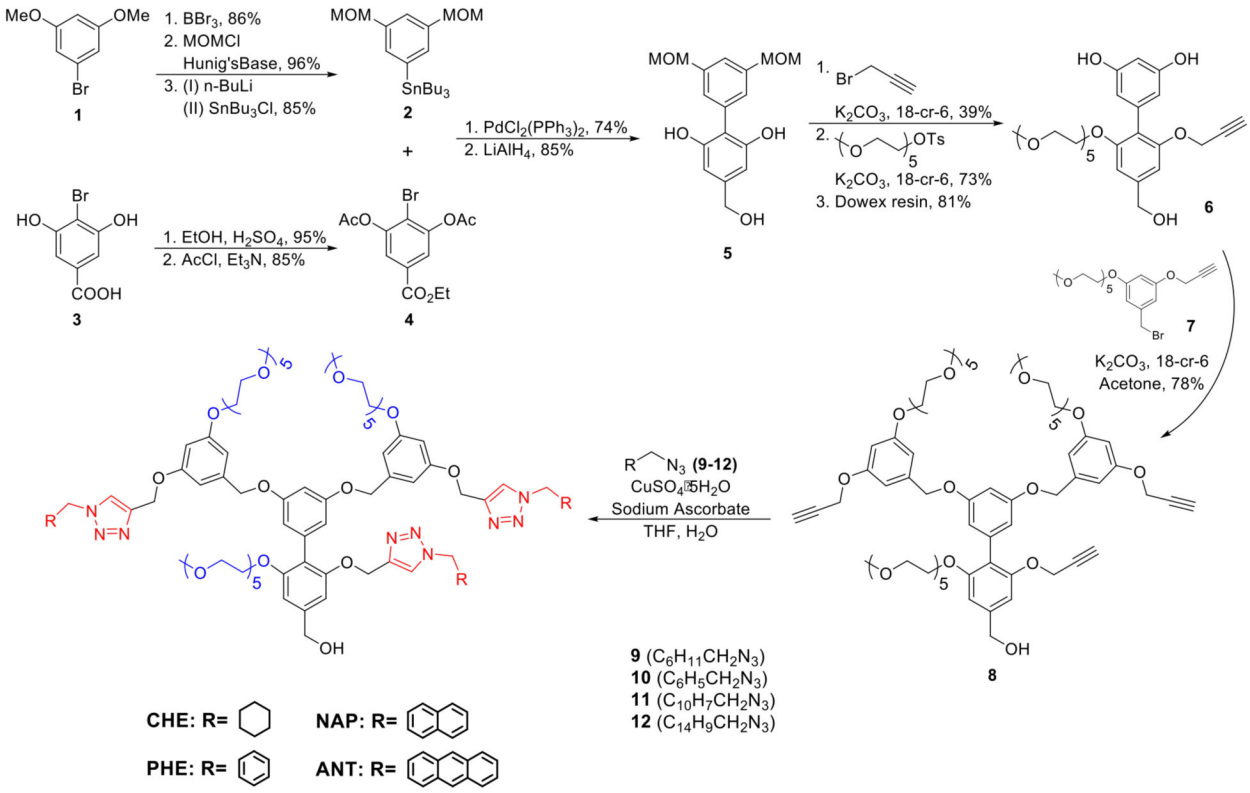

Scheme 2.

Synthesis of the targeted dendrons (**CHE**, **PHE**, **NAP** and **ANT**).

Table 1

Self-assembly enthalpies (ΔH) of all dendrons at 5°C and 25°C, and related variations (ΔΔH) expressed in kcal/mol.

Dendron	Rings[a]	ΔH(5°C)[b]	ΔH(25°C)[b]	$\Delta\Delta H = \Delta H$(25°C) − ΔH(5°C)[c]
CHE	1s	−107.3 ± 0.8	−123.3 ± 0.9	−16 ± 1.2
PHE	1a	−91.1 ± 0.8	−94.8 ± 0.6	−3.7 ± 1.1
NAP	2a	−92.1 ± 0.8	−93 ± 1.0	−0.9 ± 1.3
ANT	3a	−95 ± 0.7	−94.4 ± 0.6	0.6 ± 0.9

[a] Number of rings per-hydrophobic groups (“s”: saturated; “a”: aromatic).

[b] Self-assembly enthalpy ΔH is calculated as the sum of solute-solute and solute-solvent interactions and is expressed in kcal/mol.

[c] $\Delta\Delta H$ provides a measurement of temperature sensitivity of the assemblies. All energies values are provided as average ± standard error.

Table 2

Tail contribution to self-assembly. The tail-tail interaction free energy (ΔE_{tail}) for all dendrons at 5°C and 25°C is expressed in kcal/mol. ΔE_{tail} is also decomposed further into tail-tail stacking interaction (ΔE_{stack}) and tail-tail hydrophobic interaction (ΔE_{hyd}).

Dendron	ΔE_{tail}[a] (5°C)	ΔE_{tail}[a] (25°C)	ΔE_{stack}[b] (5°C)	ΔE_{stack}[b] (25°C)	ΔE_{hyd}[c] (5°C)	ΔE_{hyd}[c] (25°C)
CHE	−38.9	−44.1	−13.6 (35%)	−11.8 (27%)	−25.3 (65%)	−32.3 (73%)
PHE	−49.6	−50.4	−42.9 (86%)	−43.4 (86%)	−6.8 (14%)	−6.9 (14%)
NAP	−49.7	−49.2	−46.3 (93%)	−47.5 (97%)	−3.4 (7%)	−1.7 (3%)
ANT	−57.6	−55.9	−56.3 (98%)	−55.1 (98%)	−1.3 (2%)	−0.8 (2%)

[a] ΔE_{tail} values are extracted from the *g(r)* (see SI).

[b] ΔE_{stack} values are evaluated from the number of stably stacked tail groups in the assemblies multiplied for the stacking interaction energies of **CHE**, **PHE**, **NAP** and **ANT** groups.[46]

[c] ΔE_{hyd} is calculated as the difference between ΔE_{tail} and ΔE_{stack}. All energies are expressed in kcal/mol.